PHYSICAL REVIEW A **90**, 053423 (2014)

Ab initio non-Born-Oppenheimer simulations of rescattering dissociation of H_2 in strong infrared laser fields

Zhi-Chao Li[1] and Feng He[1,2,*]

[1]*Key Laboratory for Laser Plasmas (Ministry of Education) and Department of Physics, Shanghai Jiaotong University, Shanghai 200240, China*

[2]*State Key Laboratory of Precision Spectroscopy, East China Normal University, Shanghai 200062, China*

(Received 25 July 2014; published 20 November 2014)

We simulate the time-dependent Schrödinger equation and observe the rescattering dissociation of H_2 in strong infrared laser fields. Two dissociation pathways are identified, i.e., the dissociation of H_2^+ in the $2p\sigma_u$ state and the dissociation of H_2 in doubly excited states. The former accounts for larger proportions as the rescattering energy is larger. The kinetic energy release of dissociative fragments reflects the temporal internuclear distance at the moment the rescattering happens.

DOI: 10.1103/PhysRevA.90.053423 PACS number(s): 32.80.Rm, 32.30.Jc, 34.80.Qb, 42.65.Ky

I. INTRODUCTION

Rescattering is the central process in strong field physics [1,2]. In this scenario, an electron tunneling out the laser-dressed Coulomb potential, followed by the acceleration in strong laser fields, may recollide with its parent ion once laser fields change directions [3]. Rescattering usually accompanies several intriguing phenomena, such as high-order-harmonic generation [4,5], double ionization [6,7], and dissociation [8]. The last one constitutes the main topic of this paper.

As the simplest neutral molecule, H_2 works as a prototype for studying the rescattering dissociation in strong infrared laser pulses. The rescattering dissociation of H_2 is sketched in Fig. 1(a). When H_2 is exposed to strong laser fields, one electron detaches from the nuclei and the generated H_2^+ starts to stretch, since the molecular bond becomes weaker due to the loss of one electron. When the freed electron is sent back by the driving laser field, it may excite H_2^+ from the bound $1s\sigma_g$ state to the repulsive $2p\sigma_u$ state, followed by molecular dissociation. If the rescattering energy is not big enough to induce such a transition, alternatively, the freed electron may combine with H_2^+, forming a neutral H_2 in doubly excited states. Rescattering dissociation has been experimentally observed in D_2 [8,9], CO_2^+ [10], CO [11,12], O_2 [13], and polyatomic molecules [14]. By checking the kinetic energy release (KER), rescattering dissociation can be well distinguished from bond softening [15,16] and above-threshold dissociation [17]. Since rescattering only happens when the driving laser field is linearly polarized, rescattering dissociation can be confirmed by comparing the signals obtained from linearly and elliptically polarized laser pulses [18]. The dissociating H_2^+ may further be ionized, resulting in Coulomb explosion [19,20].

Martín *et al.* have calculated the dissociative ionization of H_2 and D_2 to very high accuracies, which have been quantitatively compared with experimental measurements, and discovered some molecular dynamics in attosecond time scales [21–25]. However, the *ab initio* non-Born-Oppenheimer simulations of rescattering dissociation of molecules in strong infrared laser pulses are still missing in spite of the fact that the rescattering dissociation has been confirmed experimentally for more than a decade. Several theoretical methods are invented to circumvent the electron-electron-nuclei correlation relating to rescattering dissociation. Gräfe and Ivanov [26] used an effective interaction potential to describe the rescattering excitation. de Vivie-Riedle *et al.* [27,28] separated electrons and nuclei under the Born-Oppenheimer approximation for propagation in each eigenstate base. Such a method has also been applied by Hu *et al.* [29]. Tong *et al.* used the molecular Ammosov-Delone-Krainov approximation to describe the tunneling step, followed by the classical trajectory calculations of acceleration and rescattering [30]. Different theoretical treatments lead to different explanations for experimental measurements [31–33].

In this paper, we directly simulate the non-Born-Oppenheimer time-dependent Schrödinger equation (TDSE) for H_2 in reduced dimensionality. Rescattering dissociation is clearly demonstrated in our calculations. Simulation results show that even if the rescattering energy is smaller than the critical energy required to trigger the excitation estimated from classical theories, considerable rescattering dissociation may still happen attributed to the widely spatial distribution of nuclear wave packets. The rescattering electron can be used to read the temporal dynamics of the nuclear wave packet formed in the first ionization in attosecond time scales.

II. NUMERICAL MODEL

The governed TDSE for H_2 is written as (atomic units, $e = m = \hbar = 1$, are used unless indicated otherwise)

$$i\frac{\partial}{\partial t}\Psi(R,x_1,x_2;t) = [T + V(R,x_1,x_2)]\Psi(R,x_1,x_2;t), \quad (1)$$

with the kinetic operator

$$T = \frac{p_R^2}{2\mu} + \frac{[p_1 + A(t)]^2}{2} + \frac{[p_2 + A(t)]^2}{2}, \quad (2)$$

and the potential

$$V(R,x_1,x_2) = \frac{1}{R} + \frac{1}{\sqrt{(x_1 - x_2)^2 + \alpha(R)}} - \sum_{s=\pm1}\sum_{i=1}^{2} \times \frac{1}{\sqrt{(x_i + sR/2)^2 + \frac{\beta(R)^2}{25}} + \frac{1}{\beta(R)} - \frac{\beta(R)}{5}}. \quad (3)$$

*fhe@sjtu.edu.cn

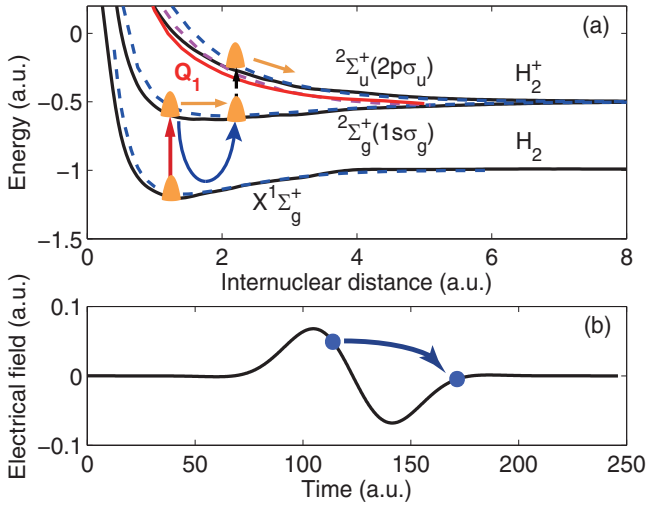

FIG. 1. (Color online) (a) Calculated potential energy surfaces of H_2 and H_2^+ (solid curves). The dashed curves obtained from [35,36] are shown for comparison. The single ionization of H_2 gives birth to H_2^+, which will stretch and then be excited to $2p\sigma_u$ by rescattering electron wave packets, followed by molecular dissociation. (b) The laser field used in the simulations.

In Eq. (2), μ is the reduced nuclear mass, and $A(t)$ is the laser vector potential and $A(t) = -\int_0^t E(t')dt'$ with $E(t)$ being the electric field. p_R, p_1, and p_2 are the relative nuclear momentum operator, and the first and second electron momentum operators, respectively. The R-dependent soft core parameter $\alpha(R)$ and $\beta(R)$ [34] are adjusted for producing the potential surfaces, shown by the solid curves in Fig. 1(a). For reference, the actual potential curves [35,36] are also shown by dashed curves. The four potential curves from bottom to top are respectively for the ground state of H_2 ($X\,^1\Sigma_g^+$), the ground state of H_2^+ ($^2\Sigma_g^+$), the doubly excited state of H_2 (Q_1, $^1\Sigma_u^+$), and the first excited state of H_2^+ ($^2\Sigma_u^+$). The comparison of solid and dashed curves shows that our reduced-dimensional model can describe the main physics well. In simulations, spatial grids are $\Delta x_1 = \Delta x_2 = 0.3$ and $\Delta R = 0.04$, and the time step is $\Delta t = 0.2$. Simulation convergences have been tested by using denser time-spatial grids. The ground-state $X\,^1\Sigma_g^+$ energy is -1.2 atomic units (a.u.), and the equilibrium internuclear distances of H_2 and H_2^+ are 1.3 a.u. and 2 a.u., respectively. Because of spin selection rules, the transition between $X\,^1\Sigma_g^+$ and the first excited state of H_2 ($^3\Sigma_u^+$, not shown) is prohibited. The energy gap between $1s\sigma_g$ and $2p\sigma_u$ at $R = 2$ is 0.4 a.u. In the following simulations, we adopt a three-dimensional simulation box $x_1 - x_2 - R$ having the grids $3000 \times 3000 \times 250$, which is large enough that no dissociative wave packets reach numerical boundaries during whole simulations. Some ionized wave packets are absorbed in simulation boundaries by a mask function [37]. The similar numerical model has been used to study the double ionization of H_2 [38,39] and high-order-harmonic generation [40].

To watch the rescattering dissociation clearly, we expose H_2 to an ultrashort laser pulse, as shown in Fig. 1(b), which is expressed as

$$E(t) = E_0 \cos(\omega t) e^{-4\ln 2\,(t/\tau - 1/2)^2}, \qquad (4)$$

where τ equals half an optical cycle, and $\omega = 0.057$ a.u., corresponding to a laser pulse with a wavelength of 800 nm. Rescattering happens only once in such an ultrashort laser pulse. As sketched in Fig. 1(b), according to the classical estimation, the electron tunneling out at $t = 115$ a.u. will gain the maximum rescattering energy at $t = 175$ a.u. In this paper, we limit the IR laser intensity such that the rescattering energy is too small to induce nonsequential double ionization [38,39].

III. SIMULATION RESULTS

Following the wave-function propagation (see Ref. [41] for a supplemental movie), one may analyze all physical processes triggered by the laser pulse. Figure 2 shows the snapshots of wave-function distribution in $x_1 - R$ space $W(x_1, R) = \int dx_2 |\Psi(R, x_1, x_2; t)|^2$ at (a) $t = 120$, (b) $t = 168$, (c) $t = 240$, and (d) $t = 324$ a.u. In (a), one may see the first half optical cycle pulls out the electron along the $-x$ axis, at the same time, H_2^+ with bound nuclear vibrational states is formed. This ejected electron wave packet is sent back to the nuclei by the second half optical cycle, as shown in (b), where the rescattering between the freed electron and H_2^+ already happens. In (c), besides the single ionization, we observe the part distributed in the area with a relative larger R. This part continuously propagates towards the area with even larger R, as shown in (d) marked by the dotted rectangle. We identify this part as molecular dissociation. The electron wave packets ejected around two optical peaks superimpose, resulting in the intracycle interference [42–44]. The corresponding interference pattern may be clearly seen in the dashed rectangle in the panel (d). We parenthetically point out that the photon energy is shared by the photoelectron and the nuclear vibration in the single ionization of H_2 [45]. The wave-function propagation movie in the Supplemental Material [41] may show more details about the rescattering

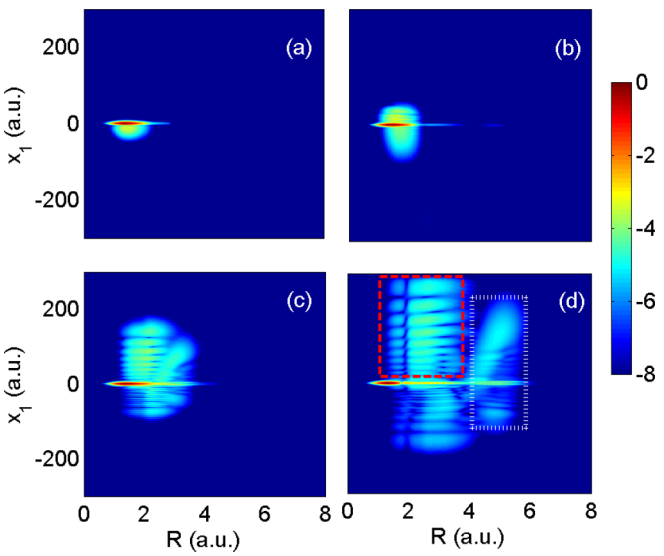

FIG. 2. (Color online) The snapshots of wave-packet distribution in $x_1 - R$ space at (a) $t = 120$, (b) $t = 168$, (c) $t = 240$, and (d) $t = 324$ a.u. in logarithm scale. The single ionization with bound H_2^+ and rescattering dissociation in (d) are marked by dashed and dotted rectangles. The laser intensity is 4×10^{14} W/cm^2.

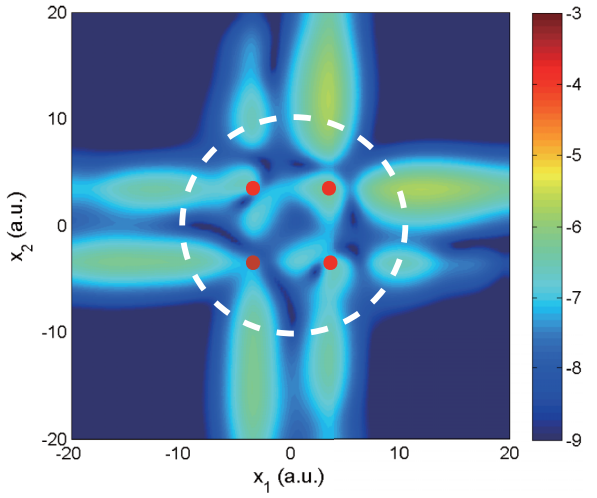

FIG. 3. (Color online) The snapshot of wave-packet distribution in $x_1 - x_2$ space at $t = 456$ a.u. in logarithm scale. The internuclear distance is $R = 7$. The dashed circle with the radius $R = \sqrt{x_1^2 + x_2^2} = 10$ is used to distinguish the doubly excited state of H_2 and the ionized dissociative state of $H_2{}^+$. The four dots represent the nuclear positions.

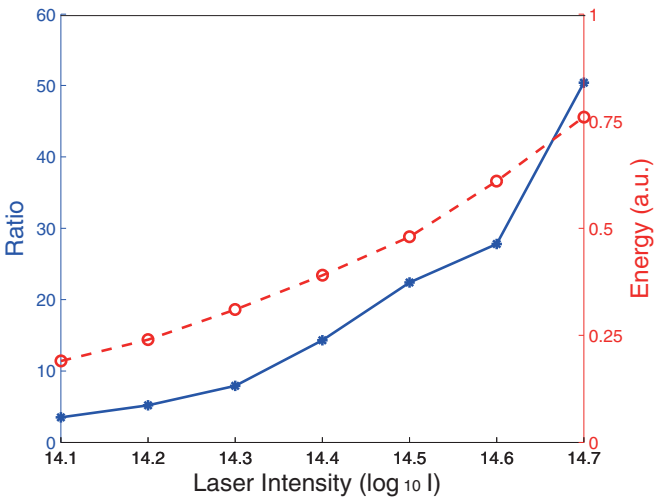

FIG. 4. (Color online) The probability ratio of ionized dissociative $H_2{}^+$ and doubly excited H_2 (solid line with stars), as well as the the rescattering energy (dashed line with open circles), as a function of laser intensities.

dissociation. Most rescattering electron wave packets finally propagate along the $+x_{1,2}$ axis, which is in coincidence with classical expectation. A very small part of the rescattering dissociation displayed in the lower half space is attributed to the back rescattering [46].

The rescattering-induced dissociation channels may be extracted by capturing the wave-packet distribution in $x_1 - x_2$ space. Figure 3 shows $|\Psi(x_1, x_2, R = 7)|^2$ at $t = 456$ a.u., when the mainly dissociating wave packet is passing through $R = 7$ a.u. The four dots in Fig. 3 represent nuclear positions, and the circle with a radius $\sqrt{x_1^2 + x_2^2} = 10$ is used to roughly distinguish two dissociation channels. In the area $\sqrt{x_1^2 + x_2^2} > 10$, one electron is ionized and the other one has the maximum distribution on the lines $x_{1,2} = \pm 3.5$, which confirms that the bounded electron in the dissociating $H_2{}^+$ is in an atomic ground state, and thereby $H_2{}^+$ is dissociating along the $2p\sigma_u$ potential curve. On the contrary, in the inner part ($\sqrt{x_1^2 + x_2^2} < 10$), both electrons are bound. The electron probabilities on points $x_1 = -x_2 = \pm 3.5$ are very small, indicating neither electron is in the atomic $1s$ state, and thereby H_2 in doubly excited states is formed. The asymmetric distribution on $x_1 = x_2 = \pm 3.5$ shows a temporary H^-H^+ is formed, which has been mentioned before [38]. The temporary H^-H^+ may be regarded as the superposition of several doubly excited states of H_2. Due to the electron-electron correlation, the doubly excited H_2 slowly decays into dissociative $H_2{}^+$ plus a free electron [24].

To further confirm the above molecular dissociation is indeed caused by electron rescattering instead of by the laser directly excitation, we omit the laser action on the second electron [in Eq. (2)] and therefore the only way to excite the second electron is the rescattering excitation. By doing that, we have observed similar molecular dissociation and the dissociation probability is reduced by half, as well as the ionization probability.

The two dissociation channels described in Fig. 3 depend on rescattering energies. Since the energies of some doubly excited states of H_2 are lower than the energy of $H_2{}^+$ in $2p\sigma_u$ at a same internuclear distance, the dissociation through doubly excited H_2 will have larger proportion if the rescattering energy is smaller. Figure 4 plots the ratio of probabilities for dissociating $H_2{}^+$ and for doubly excited H_2, as well as the maximum rescattering energy, as a function of laser intensities. Here the maximum rescattering energies are calculated by solving the Newtonian equation. The probabilities are counted by integrating the probabilities distributed within or out of the ring $\sqrt{x_1^2 + x_2^2} = 10$ just after all the dissociative wave packets propagate into the area $R > 7$. As expected, the ratio increases with the increase of rescattering energies. Even though the rescattering energy is not big enough to conquer the energy gap between $1s\sigma_g$ and $2p\sigma_u$ at the equilibrium internuclear distance, $H_2{}^+$ can still be excited to $2p\sigma_u$ because the nuclear wave packets have wide spatial distribution.

One may note that the lifetime of the doubly excited H_2 is only a few femtoseconds [47,48]. Hence, a part of doubly excited H_2 has already decayed into $H_2{}^+$ plus a free electron before the internuclear distance increases to 7 a.u. Therefore the dissociation through doubly excited H_2 in Fig. 4 is underestimated.

Once H_2 is tunneling ionized, $H_2{}^+$ starts to relax and the internuclear distance increases. The time interval between the tunneling ionization and rescattering directly relates to laser periods or laser wavelengths. For longer wavelengths, $H_2{}^+$ has longer time to relax before it is excited to $2p\sigma_u$; therefore the rescattering dissociation will start from a larger internuclear distance and finally dissociative fragments gain smaller KER. Figure 5(a) shows KER spectra when driving laser fields with different wavelengths are applied. The intensities for 600, 800, 1000, 1200, and 1600 nm pulses are 7.5×10^{14}, 4×10^{14}, 2.5×10^{14}, 1.7×10^{14}, and 1×10^{14} W/cm^2, respectively, for ensuring the corresponding maximum rescattering energies are all 0.6 a.u. As expected, the peaks of KER spectra shift

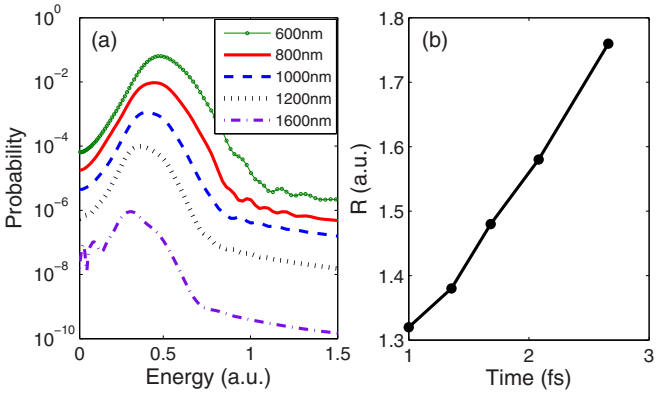

FIG. 5. (Color online) (a) The KER spectra when laser fields with different wavelengths are applied. The laser intensities for 600, 800, 1000, 1200, and 1600 nm pulses are 7.5×10^{14}, 4×10^{14}, 2.5×10^{14}, 1.7×10^{14}, and 1×10^{14} W/cm^2, respectively. (b) The calibrated time-resolved internuclear distance.

towards lower energies as driving laser wavelengths are longer. Since the laser pulses with longer wavelengths trigger smaller ionization probabilities, the total rescattering dissociation probabilities decline when wavelengths increase. Even when the rescattering energy is quite small, considerable rescattering dissociation may still happen. Therefore we support the explanation in [33] that the first rescattering has been used to read the molecular dynamics in attosecond time scales.

KER spectra can be used to calibrate the internuclear distance at the moment of rescattering, considering the fact that $2E_{\mathrm{KER}} = E_{1s\sigma_g}(1.3) - E_{1s\sigma_g}(R) + E_{2p\sigma_u}(R) - E_{2p\sigma_u}(\infty)$ (we assume the dissociation along $2p\sigma_u$ is dominated), where R is the internuclear distance where dissociation starts, and $E_{1s\sigma_g}(R)$ and $E_{2p\sigma_u}(R)$ are potential energies of $1s\sigma_g$ and $2p\sigma_u$ states at R. Recall that 1.3 a.u. is the equilibrium internuclear distance of H_2. Figure 5(b) plots the calibrated internuclear distance as a function of time intervals between ionization and rescattering. Here, the time intervals are two-thirds of laser periods. As already demonstrated experimentally by Niikura *et al.* [33], we are able to read the time-resolved internuclear distance.

IV. CONCLUSIONS

In conclusion, we demonstrate the rescattering dissociation of H_2 in strong laser fields by *ab initio* non-Born-Oppenheimer quantum simulations. Two dissociation channels are identified, i.e., the dissociation of doubly excited H_2 and the dissociation of H_2^+ along the $2p\sigma_u$ state, whereas the latter channel has a larger proportion for a larger rescattering energy. The KER spectra of rescattering dissociative fragments shift towards lower energies if the time interval between tunneling ionization and rescattering is longer. This rescattering dissociation is a platform for further studying the electron localization in the rescattering dissociation [8], charge resonance enhanced ionization [49] with moving nuclei, autoionization of the doubly excited H_2 [35], and some other ultrafast dynamics in small molecules.

ACKNOWLEDGMENTS

This work was supported by the National Natural Science Fund (Grants No. 11104180, No. 11175120, No. 11121504, and No. 11322438), and the Fok Ying-Tong Education Foundation for Young Teachers in the Higher Education Institutions of China (Grant No. 131010).

[1] P. B. Corkum, Phys. Today **64**, 36 (2011).
[2] F. Krausz and M. Ivanov, Rev. Mod. Phys. **81**, 163 (2009).
[3] P. B. Corkum and F. Krausz, Nat. Phys. **3**, 381 (2007).
[4] J. L. Krause, K. J. Schafer, and K. C. Kulander, Phys. Rev. Lett. **68**, 3535 (1992).
[5] P. B. Corkum, Phys. Rev. Lett. **71**, 1994 (1993).
[6] B. Walker, B. Sheehy, L. F. DiMauro, P. Agostini, K. J. Schafer, and K. C. Kulander, Phys. Rev. Lett. **73**, 1227 (1994).
[7] W. Becker, X. Liu, P. J. Ho, and J. H. Eberly, Rev. Mod. Phys. **84**, 1011 (2012).
[8] M. F. Kling, Ch. Siedschlag, A. J. Verhoef, J. I. Khan, M. Schultze, Th. Uphues, Y. Ni, M. Uiberacker, M. Drescher, F. Krausz, and M. J. J. Vrakking, Science **312**, 246 (2006).
[9] D. Ray, F. He, S. De, W. Cao, H. Mashiko, P. Ranitovic, K. P. Singh, I. Znakovskaya, U. Thumm, G. G. Paulus, M. F. Kling, I. V. Litvinyuk, and C. L. Cocke, Phys. Rev. Lett. **103**, 223201 (2009).
[10] J. McKenna, M. Suresh, B. Srigengan, I. D. Williams, W. A. Bryan, E. M. L. English, S. L. Stebbings, W. R. Newell, I. C. E. Turcu, J. M. Smith, E. J. Divall, C. J. Hooker, A. J. Langley, and J. L. Collier, Phys. Rev. A **74**, 043409 (2006).
[11] I. Znakovskaya, P. von den Hoff, S. Zherebtsov, A. Wirth, O. Herrwerth, M. J. J. Vrakking, R. de Vivie-Riedle, and M. F. Kling, Phys. Rev. Lett. **103**, 103002 (2009).
[12] Y. Liu, X. Liu, Y. Deng, C. Wu, H. Jiang, and Q. Gong, Phys. Rev. Lett. **106**, 073004 (2011).
[13] X. Liu, C. Wu, Z. Wu, Y. Liu, Y. Deng, and Qihuang Gong, Phys. Rev. A **83**, 035403 (2011).
[14] X. Xie, K. Doblhoff-Dier, S. Roither, M. S. Schöffler, D. Kartashov, H. Xu, T. Rathje, G. G. Paulus, A. Baltuska, Stefanie Gräfe, and M. Kitzler, Phys. Rev. Lett. **109**, 243001 (2012).
[15] A. D. Bandrauk and M. L. Sink, J. Chem. Phys. **74**, 1110 (1981).
[16] P. H. Bucksbaum, A. Zavriyev, H. G. Muller, and D. W. Schumacher, Phys. Rev. Lett. **64**, 1883 (1990).
[17] A. Giusti-Suzor, X. He, O. Atabek, and F. H. Mies, Phys. Rev. Lett. **64**, 515 (1990).
[18] H. Niikura, F. Legare, R. Hasbani, A. D. Bandrauk, Misha Yu. Ivanov, D. M. Villeneuve, and P. B. Corkum, Nature (London) **417**, 917 (2002).
[19] C. Beylerian, S. Saugout, and C. Cornaggia, J. Phys. B **39**, L105 (2006).
[20] F. Legare, I. A. Bocharova, P. Lassonde, R. Karimi, J. H. Sanderson, T. Johnston, J. Kieffer, and I. V. Litvinyuk, J. Phys. B **42**, 235601 (2009).
[21] G. Sansone, F. Kelkensberg, J. F. Pérez-Torres, F. Morales, M. F. Kling, W. Siu, O. Ghafur, P. Johnsson, M. Swoboda, E. Benedetti, F. Ferrari, F. Lépine, J. L. Sanz-Vicario, S. Zherebtsov, I. Znakovskaya, A. L'Huillier, M. Yu. Ivanov, M.

Nisoli, F. Martín, and M. J. J. Vrakking, Nature (London) **465**, 763 (2010).
[22] F. Kelkensberg, W. Siu, J. F. Pérez-Torres, F. Morales, G. Gademann, A. Rouzée, P. Johnsson, M. Lucchini, F. Calegari, J. L. Sanz-Vicario, F. Martín, and M. J. J. Vrakking, Phys. Rev. Lett. **107**, 043002 (2011).
[23] A. González-Castrillo, A. Palacios, F. Catoire, H. Bachau, and F. Martín, J. Phys. Chem. A **116**, 2704 (2012).
[24] A. Fischer, A. Sperl, P. Cörlin, M. Schönwald, H. Rietz, A. Palacios, A. González-Castrillo, F. Martín, T. Pfeifer, J. Ullrich, A. Senftleben, and R. Moshammer, Phys. Rev. Lett. **110**, 213002 (2013).
[25] P. Ranitovic, C. W. Hogle, P. Riviére, A. Palacios, X.-M. Tong, N. Toshima, A. González-Castrillo, L. Martin, F. Martín, M. M. Murnane, and H. Kapteyn, Proc. Natl. Acad. Sci. USA **111**, 912 (2013).
[26] S. Grafe and M. Y. Ivanov, Phys. Rev. Lett. **99**, 163603 (2007).
[27] D. Geppert, P. von den Hoff, and R. de Vivie-Riedle, J. Phys. B **41**, 074006 (2008).
[28] M. F. Kling, P. von den Hoff, I. Znakovskaya and R. de Vivie-Riedle, Phys. Chem. Chem. Phys. **15**, 9448 (2013).
[29] J. Hu, K. L. Han, and G. Z. He, Phys. Rev. Lett. **95**, 123001 (2005).
[30] X. M. Tong, Z. X. Zhao, and C. D. Lin, Phys. Rev. Lett. **91**, 233203 (2003).
[31] X. M. Tong, Z. X. Zhao, and C. D. Lin, Phys. Rev. Lett. **97**, 049301 (2006).
[32] Jie Hu, Ke-Li Han, and Guo-Zhong He, Phys. Rev. Lett. **97**, 049302 (2006).
[33] H. Niikura, F. Legare, R. Hasbani, M. Yu. Ivanov, D. M. Villeneuve, and P. B. Corkum, Nature (London) **421**, 826 (2003).
[34] B. Feuerstein and U. Thumm, Phys. Rev. A **67**, 043405 (2003).
[35] F. Martín, J. Fernández, T. Havermeier, L. Foucar, Th. Weber, K. Kreidi, M. Schöffler, L. Schmidt, T. Jahnke, O. Jagutzki, A. Czasch, E. P. Benis, T. Osipov, A. L. Landers, A. Belkacem, M. H. Prior, H. Schmidt-Böcking, C. L. Cocke, and R. Dörner, Science **315**, 629 (2007).
[36] T. E. Sharp, At. Data **2**, 119 (1971).
[37] F. He, C. Ruiz, and A. Becker, Phys. Rev. Lett. **99**, 083002 (2007).
[38] S. Saugout, C. Cornaggia, A. Suzor-Weiner, and E. Charron, Phys. Rev. Lett. **98**, 253003 (2007).
[39] S. Saugout, E. Charron, and C. Cornaggia, Phys. Rev. A **77**, 023404 (2008).
[40] A. D. Bandrauk, S. Chelkowski, and H. Lu, J. Phys. B **42**, 075602 (2009).
[41] See Supplemental Material at http://link.aps.org/supplemental/10.1103/PhysRevA.90.053423 for the molecular wavefunction propagation.
[42] R. Gopal, K. Simeonidis, R. Moshammer, Th. Ergler, M. Dürr, M. Kurka, K.-U. Kühnel, S. Tschuch, C.-D. Schröter, D. Bauer, J. Ullrich, A. Rudenko, O. Herrwerth, Th. Uphues, M. Schultze, E. Goulielmakis, M. Uiberacker, M. Lezius, and M. F. Kling, Phys. Rev. Lett. **103**, 053001 (2009).
[43] D. G. Arbo, K. L. Ishikawa, K. Schiessl, E. Persson, and J. Burgdörfer, Phys. Rev. A **81**, 021403(R) (2010).
[44] Ming-Hui Xu, Liang-You Peng, Zheng Zhang, Qihuang Gong, Xiao-Min Tong, Evgeny A. Pronin, and Anthony F. Starace, Phys. Rev. Lett. **107**, 183001 (2011).
[45] C. B. Madsen, F. Anis, L. B. Madsen, and B. D. Esry, Phys. Rev. Lett. **109**, 163003 (2012).
[46] T. Morishita, A. T. Le, Z. Chen, and C. D. Lin, Phys. Rev. Lett. **100**, 013903 (2008).
[47] I. Sánchez and F. Martín, J. Chem. Phys. **106**, 7720 (1997).
[48] A. Fischer, A. Sperl, P. Cörlin, M. Schönwald, S. Meuren, J. Ullrich, T. Pfeifer, R. Moshammer, and A. Senftleben, J. Phys. B **47**, 021001 (2014).
[49] T. Zuo and A. D. Bandrauk, Phys. Rev. A **52**, R2511(R) (1995).